PERGAMON

International Journal of Solids and Structures 38 (2001) 3007–3020

INTERNATIONAL JOURNAL OF SOLIDS and STRUCTURES

www.elsevier.com/locate/ijsolstr

Micromechanics of composite materials using multivariable finite element method and homogenization theory

Huiyu Sun [a,b,*], Shenglin Di [a], Nong Zhang [a], Changchun Wu [b]

[a] *Faculty of Engineering, University of Technology, No 1, Broadway, Sydney, NSW 2007, Australia*

[b] *Department of Modern Mechanics, University of Science and Technology of China, Anhui 230027, People's Republic of China*

Received 22 September 1999; in revised form 18 January 2000

Abstract

A new method for evaluation of the micro-mechanical properties of composite materials via incompatible multivariable FEM and homogenization theory is proposed in this paper. An incompatible displacement element and a hybrid stress element are developed and extended to predict the effective mechanical properties of composite materials. The mechanical performances obtained by these elements are compared with the experimental data as well as the results by Mori–Tanaka theory and traditional rule-of-mixtures. It turns out that the proposed new method provides with the best results comparing to the experimental results.

Keywords: Multivariable finite element method; Homogenization theory; Incompatible element; Hybrid element; Composite materials; Mechanical properties

1. Introduction

More and more composite materials are being used in a variety of industries now. One common problem in the mechanics of composites is to establish rational microstructural model and to determine effective properties for a composite from the distribution and properties of constituent. Furthermore, the properties of a hypothetical composite could be required in order to make early design decisions and to tailor a composite for specific application.

Many researchers (Hashin, 1983) have extensively addressed the effective properties for linear elastic composites. Based on the Eshelby–Mori–Tanaka theory, Zhao and Weng (1990) derived nine effective elastic constants of an orthotropic composite reinforced with monotonically aligned elliptic cylinders, and the five elastic moduli of a transversely isotropic composite reinforced with two-dimensional randomly-oriented elliptic cylinders. These moduli are given in terms of the cross-sectional aspect ratio and the volume fraction of the elliptic cylinders. In the approach using homogenized theory developed by Lene and Leguillon (1982), Lene (1986) and Jansson (1992), a unit cell problem governing effective mechanical

* Corresponding author. Tel.: +61-2-9514-2645; fax: +61-2-9514-2633.
E-mail address: huiyu.sun@eng.uts.edu.au (H. Sun).

0020-7683/01/$ - see front matter
PII: S0020-7683(00)00218-3

properties for composites with periodic micro-structure has been derived by employing an asymptotic expansion of the field variables in two length scales. Numerical computations using a finite element method are performed on a fiber reinforced material. Since the displacement field is interpolated with isoparametric elements, selective reduced integration has to be used to avoid locking (Jansson, 1992).

The most well-known drawback of conventional method is, based on the principle of minimum potential energy, the displacement elements behave always over stiffened. In the case of a beam subjected to bending and shear, a poor computational result is obtained with the compatible element. For nearly incompressible material, the conventional displacement element fails to reasonably simulate the structural deformation. In the case of composite laminates, the continuous interlaminar shear stress is hard to attain by the displacement element (Phan and Reddy, 1985). For both theoretical research and engineering practice, it is worthwhile to devote on developing alternative approaches for both linear and nonlinear applications.

Since Pian (1964) first presented the hybrid stress element, 5β-I, the theory and application of hybrid elements have been greatly developed. Pian and Sumihara (1984) introduced the incompatible displacements into the Reissner principle and imposed the element internal equilibrium conditions in a variational sense to improve the stress expansions. A new hybrid element, 5β-II, with excellent qualities has been obtained. In the derivation, however, some perturbation treatments have to be applied. An optimizing condition for hybrid elements was offered by Wu et al. (1987), and a new approach for developing optimal stress patterns was presented. With this approach, a more general resultant element, 5β-III, was established without any treatment of experiences or perturbations. The optimized hybrid model shows a superior numerical behavior (Di et al., 1989), e.g., (1) it passed the patch test. (2) In comparison with 4-node displacement element, the presented method yields more ideal results for both stresses and displacements without any locking phenomena. (3) The optimized hybrid element is not sensitive to mesh distortion. (4) There are no false shears, no zero energy modes.

In order to overcome the intrinsic deficiency of isoparametric finite element, in this paper, the incompatible element and hybrid element are constructed and applied to modeling the minimum repetitive unit cell of composite materials. Both of the elements can satisfy the patch test condition, and the optimized hybrid element meets the match condition for multivariable parameters of the finite element.

2. Governing equations

Considering a heterogeneous elastomer with periodic structures, it consists of two components, Fig. 1. This body has two length scales, a global length scale D that is of the order of the body size, and a local length scale d that is proportional to the wavelength of the variation of the micro-structure. The size of the unit cell is further assumed to be much smaller than the size of the body. The relation between the global coordinate system x_i for the body and the local system y_i for the minimum repeated unit cell can then be written as

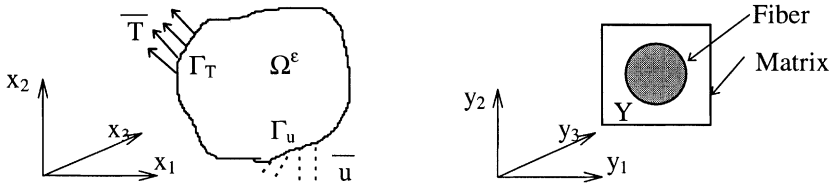

(a) elastic body Ω^ε (b) unit cell Y

Fig. 1. Elastic body and representative unit cell.

$$y_i = \frac{x_i}{\varepsilon}, \tag{1}$$

where ε is the scaling factor between the two length scales. For actual heterogeneous body, when it is subjected to external forces, the field quantities such as displacement and stress, will vary with the global coordinate system x. In the meanwhile, because of the nonlinearity of microstructure, the field quantities will vary rapidly with the neighborhood of ε within a short wavelength. The unknown stress (σ_{ij}), strain (e_{ij}) and displacement (u_i) can be solved from the equilibrium equation, geometric equation and physical equation:

$$\sigma^{\varepsilon}_{ij,j} + f_i = 0 \quad \text{in } \Omega^{\varepsilon}, \tag{2}$$

$$e^{\varepsilon}_{ij} = \tfrac{1}{2}(u^{\varepsilon}_{i,j} + u^{\varepsilon}_{j,i}) \quad \text{in } \Omega^{\varepsilon}, \tag{3}$$

$$\sigma^{\varepsilon}_{ij} = C^{\varepsilon}_{ijkl}\, e^{\varepsilon}_{kl} \quad \text{in } \Omega^{\varepsilon} \tag{4}$$

and boundary conditions

$$\sigma^{\varepsilon}_{ij} n_j = \overline{T_i} \quad \text{on } \Gamma^{\varepsilon}_T, \tag{5}$$

$$u^{\varepsilon}_i = \overline{u}_i \quad \text{on } \Gamma^{\varepsilon}_u, \tag{6}$$

where f_i is the body force, C_{ijkl} is the stiffness matrix of the material, n_j is the outward normal vector of the boundary, $\overline{T_i}$ is the given external force on the boundary Γ^{ε}_T and $\overline{u_i}$ is the given displacement on the boundary Γ^{ε}_u.

3. Asymptotic expansion

We look for an asymptotic expansion of u^{ε}_i as follows:

$$u^{\varepsilon}_i(x) = u^0_i(x,y) + \varepsilon u^1_i(x,y) + \varepsilon^2 u^2_i(x,y) + \cdots, \tag{7}$$

where the functions u^0_i, u^1_i, u^2_i, …, are Y-periodic with respect to y. The strain $e_{ij}\left(u^{\varepsilon}_i\right)$ can be expanded as

$$e_{ij}\left(u^{\varepsilon}_i\right) = \varepsilon^{-1} e^{(-1)}_{ij} + e^{(0)}_{ij} + \varepsilon e^{(1)}_{ij} + \cdots, \tag{8}$$

where

$$e^{(-1)}_{ij} = \frac{1}{2}\left(\frac{\partial u^{(0)}_i}{\partial y_j} + \frac{\partial u^{(0)}_j}{\partial y_i}\right), \tag{9}$$

$$e^{(0)}_{ij} = \frac{1}{2}\left(\frac{\partial u^{(0)}_i}{\partial x_j} + \frac{\partial u^{(0)}_j}{\partial x_i} + \frac{\partial u^{(1)}_i}{\partial y_j} + \frac{\partial u^{(1)}_j}{\partial y_i}\right), \tag{10}$$

$$e^{(1)}_{ij} = \frac{1}{2}\left(\frac{\partial u^{(1)}_i}{\partial x_j} + \frac{\partial u^{(1)}_j}{\partial x_i} + \frac{\partial u^{(2)}_i}{\partial y_j} + \frac{\partial u^{(2)}_j}{\partial y_i}\right). \tag{11}$$

Substituting the above equations into the constitutive equation (4), the expansion of the stress $\sigma^{\varepsilon}_{ij}$ can be obtained,

$$\sigma^{\varepsilon}_{ij} = \varepsilon^{-1}\sigma^{(-1)}_{ij} + \sigma^{(0)}_{ij} + \varepsilon\sigma^{(1)}_{ij} + \cdots, \tag{12}$$

where

$$\sigma_{ij}^{(-1)} = C_{ijkl}\, e_{kl}^{(-1)}(x,y), \tag{13}$$

$$\sigma_{ij}^{(0)} = C_{ijkl}\, e_{kl}^{(0)}(x,y), \tag{14}$$

$$\sigma_{ij}^{(1)} = C_{ijkl}\, e_{kl}^{(1)}(x,y). \tag{15}$$

Inserting Eq. (12) into the equilibrium equation (2), the following equations are deduced since the terms in front of ε^i should be zeros:

$$\frac{\partial \sigma_{ij}^{(-1)}}{\partial y_j} = 0, \tag{16}$$

$$\frac{\partial \sigma_{ij}^{(0)}}{\partial y_j} + \frac{\partial \sigma_{ij}^{(-1)}}{\partial x_j} = 0, \tag{17}$$

$$\frac{\partial \sigma_{ij}^{(1)}}{\partial y_j} + \frac{\partial \sigma_{ij}^{(0)}}{\partial x_j} + f_i = 0. \tag{18}$$

Using Eq. (13), Eq. (16) can be expressed as

$$\frac{\partial}{\partial y_j}\left[C_{ijkl}\, e_{kl}^{(-1)}\right] = 0. \tag{19}$$

From formulae (9) and (13), we have

$$e_{ij}^{(-1)} = 0, \qquad \sigma_{ij}^{(-1)} = 0. \tag{20}$$

From Eq. (9), $u_i^{(0)}$ is independent of y, i.e.,

$$u_i^{(0)}(x,y) = u_i^{(0)}(x). \tag{21}$$

Inserting expression (14) in Eq. (17), expression (10) can be rewritten as

$$e_{ij}^{(0)} = e_{xij}\left(u_i^{(0)}\right) + e_{yij}\left(u_i^{(1)}\right), \tag{22}$$

where

$$e_{xij}\left(u_i^{(0)}\right) = \frac{1}{2}\left(\frac{\partial u_i^{(0)}}{\partial x_j} + \frac{\partial u_j^{(0)}}{\partial x_i}\right), \qquad e_{yij}\left(u_i^{(1)}\right) = \frac{1}{2}\left(\frac{\partial u_i^{(1)}}{\partial y_j} + \frac{\partial u_j^{(1)}}{\partial y_i}\right). \tag{23}$$

Then,

$$\frac{\partial}{\partial y_j}\left[C_{ijkl}\, e_{ykl}\left(u_i^{(1)}\right)\right] = -\frac{\partial C_{ijkl}}{\partial y_j}\, e_{xkl}\left(u_i^{(0)}\right). \tag{24}$$

From the right-hand form of formula (24), $u_i^{(1)}$ may be written as

$$u_i^{(1)}(x,y) = \chi_i^{kl}(y) e_{xkl}\left(u_i^{(0)}(x)\right), \tag{25}$$

where $\chi_i^{kl}(y)$ is a Y-periodic function defined in the unit cell Y. Substituting the equation for $u_i^{(1)}$ (25) into Eq. (22), there is

$$e_{ij}^{(0)} = e_{xkl}\left(u_i^{(0)}\right)\left[T_{ij}^{kl} + e_{yij}\left(\chi_i^{kl}\right)\right], \tag{26}$$

where

$$e_{yij}\left(\chi_i^{kl}\right) = \frac{1}{2}\left(\frac{\partial \chi_i^{kl}}{\partial y_j} + \frac{\partial \chi_j^{kl}}{\partial y_i}\right). \tag{27}$$

T_{ij}^{kl} is a fourth-order unit tensor. And $T_{ij}^{kl} = 1/2\left(\delta_{ik}\delta_{jl} + \delta_{il}\delta_{jk}\right)$, where δ_{ij} is the Kronecker delta symbol. So expression (14) can be written as

$$\sigma_{ij}^{(0)} = C_{ijmn}\left[T_{mn}^{kl} + e_{ymn}\left(\chi_i^{kl}\right)\right]e_{xkl}\left(u_i^{(0)}\right). \tag{28}$$

If ε tends to be zero, the first two terms are considered in formula (12). Referring to formula (20), the stress in Ω^{ε} is

$$\sigma_{ij}^{\varepsilon} = \sigma_{ij}^{(0)} = C_{ijmn}\left[T_{mn}^{kl} + e_{ymn}\left(\chi_i^{kl}\right)\right]e_{xkl}\left(u_i^{(0)}\right). \tag{29}$$

For any Y-periodic function $\Phi = \Phi(x, y)$, the average in the domain Y is defined as follows:

$$\langle \Phi \rangle = \frac{1}{|Y|}\int_Y \Phi(x, y)\,\mathrm{d}Y. \tag{30}$$

The average of $\sigma_{ij}^{(0)}$ in the domain Y is written as

$$\left\langle \sigma_{ij}^{(0)} \right\rangle = C_{ijkl}^H e_{xkl}\left(u_i^{(0)}\right), \tag{31}$$

where

$$C_{ijkl}^H = \frac{1}{|Y|}\int_Y C_{ijmn}\left[T_{mn}^{kl} + e_{ymn}\left(\chi_i^{kl}\right)\right]\mathrm{d}Y. \tag{32}$$

The elastic constant C_{ijkl}^H defined above is independent of y. It is called homogenized equivalent elastic constant.

4. Finite element method implementation

To obtain the homogenized elastic constant, it is necessary to solve for χ_i^{kl}, which is satisfied with equation (24), i.e.,

$$\frac{\partial}{\partial y_j}\left[C_{ijkl}\, e_{ykl}\left(\chi_i^{kl}\right)\right] + \frac{\partial}{\partial y_j}\left(C_{ijkl}\right) = 0. \tag{33}$$

It is evident that χ_i^{kl} is generalized displacement, and $\partial/\partial y_j\left(C_{ijkl}\right)$ is generalized force.

$$\int_Y \frac{\partial}{\partial y_j}\left[C_{ijkl}\, e_{ykl}\left(\chi_i^{kl}\right) + C_{ijkl}\right]\varphi\,\mathrm{d}Y = 0 \quad \forall \varphi \in \Omega. \tag{34}$$

Eq. (34) can be integrated by decomposition, then

$$\int_Y \frac{\partial}{\partial y_j}\left[\left(C_{ijkl}\, e_{ykl}\left(\chi_i^{kl}\right) + C_{ijkl}\right)\varphi\right]\mathrm{d}Y - \int_Y \left[C_{ijkl}\, e_{ykl}\left(\chi_i^{kl}\right) + C_{ijkl}\right]\frac{\partial \varphi}{\partial y_j}\,\mathrm{d}Y = 0. \tag{35}$$

Use of the divergence theorem gives

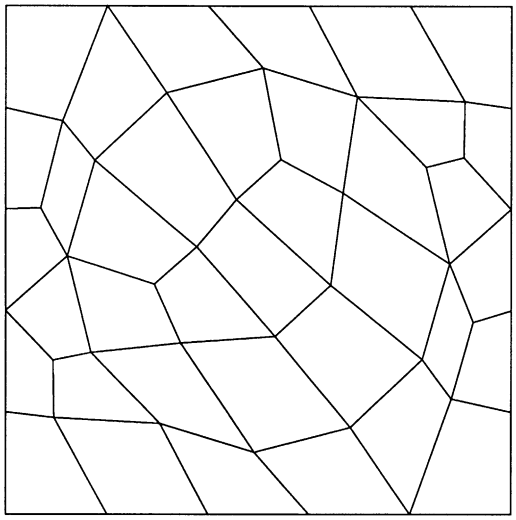

Fig. 2. Finite element mesh on a unit cell.

$$\int_Y \left[C_{ijkl}\, e_{ykl}\left(\chi_i^{kl}\right) + C_{ijkl}\right] e_{ij}(\varphi)\,\mathrm{d}Y = 0, \tag{36}$$

i.e.,

$$\int_Y C_{ijkl}\, e_{ykl}\left(\chi_i^{kl}\right) e_{ij}(\varphi)\,\mathrm{d}Y = -\int_Y C_{ijkl}\, e_{ij}(\varphi)\,\mathrm{d}Y. \tag{37}$$

For the case of two dimensions, the unit cell of composite materials is idealized as shown in Fig. 2. It is meshed by quadrilateral elements with four corner nodes.

4.1. Isoparametric finite element

With the isoparametric element adopted, the displacement in the element is interpolated as the function of nodal displacements.

$$\boldsymbol{u} = \sum_{i=1}^{4} N_i \boldsymbol{u}_i, \tag{38}$$

where N_i is the shape function. Imposing the geometric relation upon expression (25) induces

$$\boldsymbol{e}\left(\boldsymbol{u}^{(1)}\right) = \boldsymbol{e}(\chi)\boldsymbol{e}\left(\boldsymbol{u}^{(0)}\right), \tag{39}$$

$\boldsymbol{e}(\chi)$ is equivalent to generalized strain:

$$\boldsymbol{e}(\chi) = \boldsymbol{B}\boldsymbol{q}, \tag{40}$$

where $\boldsymbol{B}$ is the strain matrix, and $\boldsymbol{q}$ is the nodal displacement of the element.

From formula (37), the discrete equation for finite element can be written as follows:

$$\boldsymbol{K}\boldsymbol{q} = \boldsymbol{P}, \tag{41}$$

where

$$\boldsymbol{K} = \int_{-1}^{1}\int_{-1}^{1} \boldsymbol{B}^T \boldsymbol{C}\boldsymbol{B} h J \,\mathrm{d}\xi\,\mathrm{d}\eta, \tag{42}$$

$$\boldsymbol{P} = -\int_{-1}^{1}\int_{-1}^{1} \boldsymbol{B}^T \boldsymbol{C} h J \,\mathrm{d}\xi\,\mathrm{d}\eta, \tag{43}$$

and h is the thickness of the element, J is the determinant of Jacobian matrix.

4.2. Incompatible finite element

Based upon the general formulation of incompatible functions (Wu et al., 1987), the NQ6 incompatible element is generated and adopted in this paper. The incompatible parts of the displacement are introduced as follows:

$$\boldsymbol{u} = \begin{Bmatrix} u \\ v \\ w \end{Bmatrix} = \begin{bmatrix} N_1\boldsymbol{I}_3 & N_2\boldsymbol{I}_3 & N_3\boldsymbol{I}_3 & N_4\boldsymbol{I}_3 \end{bmatrix} \begin{Bmatrix} u_1 \\ v_1 \\ w_1 \\ \vdots \\ v_4 \\ w_4 \end{Bmatrix} + \begin{bmatrix} N_1^* & N_2^* & 0 & 0 & 0 & 0 \\ 0 & 0 & N_1^* & N_2^* & 0 & 0 \\ 0 & 0 & 0 & 0 & N_1^* & N_2^* \end{bmatrix} \begin{Bmatrix} \lambda_1 \\ \lambda_2 \\ \lambda_3 \\ \lambda_4 \\ \lambda_5 \\ \lambda_6 \end{Bmatrix}$$

$$= \boldsymbol{N}\boldsymbol{q} + \boldsymbol{N}^*\lambda, \tag{44}$$

where

$$\begin{aligned} N_1^* &= \left(1-\xi^2\right) + \frac{2}{3}\left(\frac{J_1}{J_0}\xi - \frac{J_2}{J_0}\eta\right), \\ N_2^* &= \left(1-\eta^2\right) - \frac{2}{3}\left(\frac{J_1}{J_0}\xi - \frac{J_2}{J_0}\eta\right). \end{aligned} \tag{45}$$

$\boldsymbol{I}_3$ is the third-order unit square matrix. N_1^* and N_2^* are the shape functions of incompatible displacements of the element NQ6. λ denotes displacement parameters in the element. J_0, J_1 and J_2 are parameters associated with the nodal coordinates of the element. After the geometric relation is introduced, there is

$$\boldsymbol{e} = (\boldsymbol{D}\boldsymbol{N})\boldsymbol{q} + (\boldsymbol{D}\boldsymbol{N}^*)\lambda = \boldsymbol{B}\boldsymbol{q} + \overline{\boldsymbol{B}}\lambda, \tag{46}$$

where $\boldsymbol{D}$ denotes the differential operator in the relationship between the strain and displacement. Based on the potential principle of incompatible system, formula (37) can be written in the variational form:

$$\prod_{\mathrm{p}} = \sum\left[\int_{V^{\mathrm{e}}} \left(\delta\boldsymbol{q}^{\mathrm{T}}\boldsymbol{B}^{\mathrm{T}} + \delta\lambda^{\mathrm{T}}\overline{\boldsymbol{B}}^{\mathrm{T}}\right)\boldsymbol{C}\left(\boldsymbol{B}\boldsymbol{q} + \overline{\boldsymbol{B}}\lambda\right)\mathrm{d}V + \int_{V^{\mathrm{e}}} \left(\delta\boldsymbol{q}^{\mathrm{T}}\boldsymbol{B}^{\mathrm{T}} + \delta\lambda^{\mathrm{T}}\overline{\boldsymbol{B}}^{\mathrm{T}}\right)\boldsymbol{C}\,\mathrm{d}V\right], \tag{47}$$

where V^{e} denotes the volume of every element in the domain Y. By using the extreme value condition, the following equations are derived:

$$\begin{aligned} \left(\int_{V^{\mathrm{e}}} \boldsymbol{B}^{\mathrm{T}}\boldsymbol{C}\boldsymbol{B}\,\mathrm{d}V\right)\boldsymbol{q} + \left(\int_{V^{\mathrm{e}}} \boldsymbol{B}^{\mathrm{T}}\boldsymbol{C}\overline{\boldsymbol{B}}\,\mathrm{d}V\right)\lambda &= -\int_{V^{\mathrm{e}}} \boldsymbol{B}^{\mathrm{T}}\boldsymbol{C}\,\mathrm{d}V, \\ \left(\int_{V^{\mathrm{e}}} \overline{\boldsymbol{B}}^{\mathrm{T}}\boldsymbol{C}\boldsymbol{B}\,\mathrm{d}V\right)\boldsymbol{q} + \left(\int_{V^{\mathrm{e}}} \overline{\boldsymbol{B}}^{\mathrm{T}}\boldsymbol{C}\overline{\boldsymbol{B}}\,\mathrm{d}V\right)\lambda &= -\int_{V^{\mathrm{e}}} \overline{\boldsymbol{B}}^{\mathrm{T}}\boldsymbol{C}\,\mathrm{d}V. \end{aligned} \tag{48}$$

It can be written in the form of matrix, i.e.,

$$\begin{bmatrix} \boldsymbol{K}_{qq} & \boldsymbol{K}_{q\lambda} \\ \boldsymbol{K}_{\lambda q} & \boldsymbol{K}_{\lambda\lambda} \end{bmatrix} \begin{Bmatrix} \boldsymbol{q} \\ \lambda \end{Bmatrix} = \begin{bmatrix} \boldsymbol{P}_q \\ \boldsymbol{P}_\lambda \end{bmatrix}. \tag{49}$$

From the second line of the above formula, λ can be expressed in terms of $\boldsymbol{q}$. Then, the stiffness equation of incompatible element is obtained.

$$\left(\boldsymbol{K}_{qq} - \boldsymbol{K}_{q\lambda}\boldsymbol{K}_{\lambda\lambda}^{-1}\boldsymbol{K}_{\lambda q}\right)\boldsymbol{q} = \boldsymbol{P}_q - \boldsymbol{K}_{q\lambda}\boldsymbol{K}_{\lambda\lambda}^{-1}\boldsymbol{P}_\lambda. \tag{50}$$

Considering that the equivalent nodal force of the element should not account for the effect of the incompatible shape function N^* (Wu and Pian, 1997), the stiffness equation (50) is revised.

$$\left(\boldsymbol{K}_{qq} - \boldsymbol{K}_{q\lambda}\boldsymbol{K}_{\lambda\lambda}^{-1}\boldsymbol{K}_{\lambda q}\right)\boldsymbol{q} = \boldsymbol{P}_q. \tag{51}$$

4.3. Hybrid stress element

According to the Hellinger–Reissner variational principle, the energy functional of the incompatible discrete system can be expressed as

$$\prod_{\mathrm{H-R}} = \sum \left\{ \int_{V^e} \left[-\frac{1}{2}\boldsymbol{\sigma}^{\mathrm{T}}\boldsymbol{S}\boldsymbol{\sigma} + \boldsymbol{\sigma}^{\mathrm{T}}(\boldsymbol{D}\boldsymbol{u}_q) + \boldsymbol{\sigma}_{\mathrm{h}}^{\mathrm{T}}(\boldsymbol{D}\boldsymbol{u}_\lambda) - \boldsymbol{f}(\boldsymbol{u}_q + \boldsymbol{u}_\lambda) \right] \mathrm{d}V \right\}, \tag{52}$$

where $\boldsymbol{S}$ is the compliance matrix of the element material. $\boldsymbol{u}_q$ and $\boldsymbol{u}_\lambda$ are the compatible part and incompatible part of the element displacement, respectively. $\boldsymbol{f}$ is the generalized body force that corresponds to the last term in formula (33). $\boldsymbol{\sigma}$ is the stress, which can be assumed to be the sum of constant stress $\boldsymbol{\sigma}_{\mathrm{c}}$ and higher-order stress $\boldsymbol{\sigma}_{\mathrm{h}}$, i.e.,

$$\boldsymbol{\sigma} = \begin{Bmatrix} \sigma_{11} \\ \sigma_{22} \\ \sigma_{33} \\ \sigma_{23} \\ \sigma_{31} \\ \sigma_{12} \end{Bmatrix} = \boldsymbol{I}_6 \begin{Bmatrix} \beta_1 \\ \beta_2 \\ \beta_3 \\ \beta_4 \\ \beta_5 \\ \beta_6 \end{Bmatrix} + \begin{bmatrix} \eta & 0 & 0 & 0 & 0 & 0 & \xi & 0 & 0 & 0 & 0 & 0 \\ 0 & \xi & 0 & 0 & 0 & 0 & 0 & 0 & 0 & \eta & 0 & 0 \\ 0 & 0 & \xi & \eta & 0 & 0 & 0 & 0 & 0 & 0 & 0 & 0 \\ 0 & 0 & 0 & 0 & \xi & 0 & 0 & 0 & 0 & 0 & 0 & \eta \\ 0 & 0 & 0 & 0 & 0 & \eta & 0 & 0 & 0 & 0 & \xi & 0 \\ 0 & 0 & 0 & 0 & 0 & 0 & 0 & \eta & \xi & 0 & 0 & 0 \end{bmatrix} \begin{Bmatrix} \beta_7 \\ \beta_8 \\ \beta_9 \\ \vdots \\ \beta_{17} \\ \beta_{18} \end{Bmatrix}. \tag{53}$$

The above formula can be expressed in a simple form:

$$\boldsymbol{\sigma} = \boldsymbol{\sigma}_{\mathrm{c}} + \boldsymbol{\sigma}_{\mathrm{h}} = \boldsymbol{\phi}_{\mathrm{c}}\boldsymbol{\beta}_{\mathrm{c}} + \boldsymbol{\phi}_{\mathrm{h}}\boldsymbol{\beta}_{\mathrm{h}} = \boldsymbol{\beta}_{\mathrm{c}} + [\,\phi_{\mathrm{I}} \quad \phi_{\mathrm{II}}\,] \begin{Bmatrix} \beta_{\mathrm{I}} \\ \beta_{\mathrm{II}} \end{Bmatrix}, \tag{54}$$

where ϕ_{I} and ϕ_{II} are sixth-order square matrices, $\beta_{\mathrm{I}} = [\beta_7\beta_8\cdots\beta_{12}]^{\mathrm{T}}$ and $\beta_{\mathrm{II}} = [\beta_{13}\beta_{14}\cdots\beta_{18}]^{\mathrm{T}}$.

Based on the consistency condition of incompatible hybrid element, the optimized condition for hybrid element is applied (Wu et al., 1987), i.e.,

$$\oint_{\partial V^e} \delta\boldsymbol{u}_\lambda^{\mathrm{T}}\boldsymbol{n}\boldsymbol{\sigma}_{\mathrm{h}}\,\mathrm{d}S = 0, \tag{55}$$

where ∂V^e is the element boundary and $\boldsymbol{n}$ is the outward normal vector of the element boundary. Substituting expressions (44) and (54) into Eq. (55) induces

$$\delta\lambda^{\mathrm{T}}\boldsymbol{M}\boldsymbol{\beta}_{\mathrm{h}} = 0, \tag{56}$$

where

$$\boldsymbol{M} = \oint_{\partial V^e} \boldsymbol{N}^{*\mathrm{T}}\boldsymbol{n}[\,\phi_{\mathrm{I}} \quad \phi_{\mathrm{II}}\,]\,\mathrm{d}S = [\,M_{\mathrm{I}} \quad M_{\mathrm{II}}\,], \tag{57}$$

$$M_{\mathrm{I}} = \int_{V^{\mathrm{e}}} \left[(\boldsymbol{D}\boldsymbol{N}^*)^{\mathrm{T}} \phi_{\mathrm{I}} + \boldsymbol{N}^{*T} \left(\boldsymbol{D}^{\mathrm{T}} \phi_{\mathrm{I}} \right) \right] \mathrm{d}V,$$
$$M_{\mathrm{II}} = \int_{V^{\mathrm{e}}} \left[(\boldsymbol{D}\boldsymbol{N}^*)^{\mathrm{T}} \phi_{\mathrm{II}} + \boldsymbol{N}^{*\mathrm{T}} \left(\boldsymbol{D}^{\mathrm{T}} \phi_{\mathrm{II}} \right) \right] \mathrm{d}V. \tag{58}$$

It is difficult to get the analytical form of M_{I} and M_{II}. However, they can be calculated by numerical integration, and they are functions of the nodal coordinates of the element. From Eq. (56), there is

$$[M_{\mathrm{I}} \quad M_{\mathrm{II}}] \begin{Bmatrix} \beta_{\mathrm{I}} \\ \beta_{\mathrm{II}} \end{Bmatrix} = 0, \tag{59}$$

β_{II} is expressed in terms of β_{I}. Then,

$$\boldsymbol{\sigma} = \boldsymbol{\sigma}_{\mathrm{c}} + \boldsymbol{\sigma}_{\mathrm{h}} = \boldsymbol{\beta}_{\mathrm{c}} + \boldsymbol{\phi}_{\mathrm{h}}^* \beta_{\mathrm{I}}, \tag{60}$$

where

$$\boldsymbol{\phi}_{\mathrm{h}}^* = \phi_{\mathrm{I}} - \phi_{\mathrm{II}} M_{\mathrm{II}}^{-1} M_{\mathrm{I}}. \tag{61}$$

For the hybrid element with incompatible displacement, special attention should be paid to the correlation between all variables. Better performance could be obtained if the match condition of parameters can be satisfied (Wu and Pian, 1997). Defining the number of each parameter as

$$n_q = \dim(\boldsymbol{q}), \tag{62}$$

$$n_\lambda = \dim(\lambda), \tag{63}$$

$$n_\beta = \dim(\beta), \tag{64}$$

$$n_r = \text{number of DOF of the rigid body.} \tag{65}$$

Then the match condition requires

$$n_\beta = n_q + n_\lambda - n_{\mathrm{r}}. \tag{66}$$

The proposed hybrid element obeys the above match condition and can therefore guarantee the best performance.

Substituting formula (60) into Eq. (52), the Hellinger–Reissner variational principle is rewritten as

$$\prod\nolimits^{\mathrm{e}} (\boldsymbol{\sigma}_{\mathrm{c}}, \boldsymbol{\sigma}_{\mathrm{h}}, \boldsymbol{u}_q, \boldsymbol{u}_\lambda) = \int_{V^{\mathrm{e}}} \left[-\frac{1}{2} (\boldsymbol{\sigma}_{\mathrm{c}} + \boldsymbol{\sigma}_{\mathrm{h}})^{\mathrm{T}} \boldsymbol{S} (\boldsymbol{\sigma}_{\mathrm{c}} + \boldsymbol{\sigma}_{\mathrm{h}}) + (\boldsymbol{\sigma}_{\mathrm{c}} + \boldsymbol{\sigma}_{\mathrm{h}})^{\mathrm{T}} (\boldsymbol{D}\boldsymbol{u}_q) + \boldsymbol{\sigma}_{\mathrm{h}}^{\mathrm{T}} (\boldsymbol{D}\boldsymbol{u}_\lambda) - \boldsymbol{f} (\boldsymbol{u}_q + \boldsymbol{u}_\lambda) \right] \mathrm{d}V. \tag{67}$$

From the stagnation value condition of functional (67), the stiffness equation of the hybrid element can be obtained.

5. Numerical results

In this paper, the S-2 glass-epoxy composite materials with the fiber volume fraction from 0% to 75% are used in the numerical tests. The fundamental material properties are $E_{\mathrm{f}} = 85.5$ GPa, $v_{\mathrm{f}} = 0.22$ for the S-2 glass fiber, and $E_{\mathrm{m}} = 4.1$ GPa, $v_{\mathrm{m}} = 0.34$ for the epoxy resin matrix.

The numerical results of mechanical properties achieved by using isoparametric element (denoted as iso), incompatible element (denoted as inc) and hybrid element (denoted as hyb), as well as Mori–Tanaka

method (denoted as M–T) and traditional rule-of-mixtures (denoted as rom) are shown in Figs. 3–8. A comparison can now be made between theoretical and experimental results (Lee and Mykkanen, 1987).

For the longitudinal experimental tests, fiber stresses were determined from the rule of mixtures and the measured fiber content in the specimen. These data were then averaged for all specimens. Stresses and moduli at specific fiber contents were calculated from this single set of data by the rule of mixtures. Since the test number was limitedly 31, the experimental points of major Poisson's ratio in Fig. 7 show less dependent of fiber volume fraction. For the transverse tests, not all properties were measured throughout the fiber content range of 50–70 vol.%. However, properties not measured at a fiber content of interest were obtained by statistically interpolating or extrapolating from regions, where data was available over a sufficient range. For the shear tests, specimens were cut at $\pm 45°$ from a balanced-ply, 6-layer $0°/90°$ winding. The $\pm 45°$-tensile shear test was used to determine in-plane shear properties (Clements and Moore, 1979).

Fig. 3 illustrates that there is a difference between the numerical results by hyb, inc, iso and those by M–T, rom. The numerical results by hyb, inc and iso show better agreement with the experimental result than those by M–T and rom. Fig. 4 shows that the transverse moduli by hyb, inc and iso are closer to the experimental result than those by M–T and rom. The numerical result by hyb is the fittest to the experimental result. In Fig. 5, the numerical results by hyb, inc and iso are better than that by M–T. The similar conclusion can be attained from Fig. 6. Figs. 7 and 8 illustrate major Poisson's ratio and transverse shear modulus with the variation of fiber volume fraction, respectively.

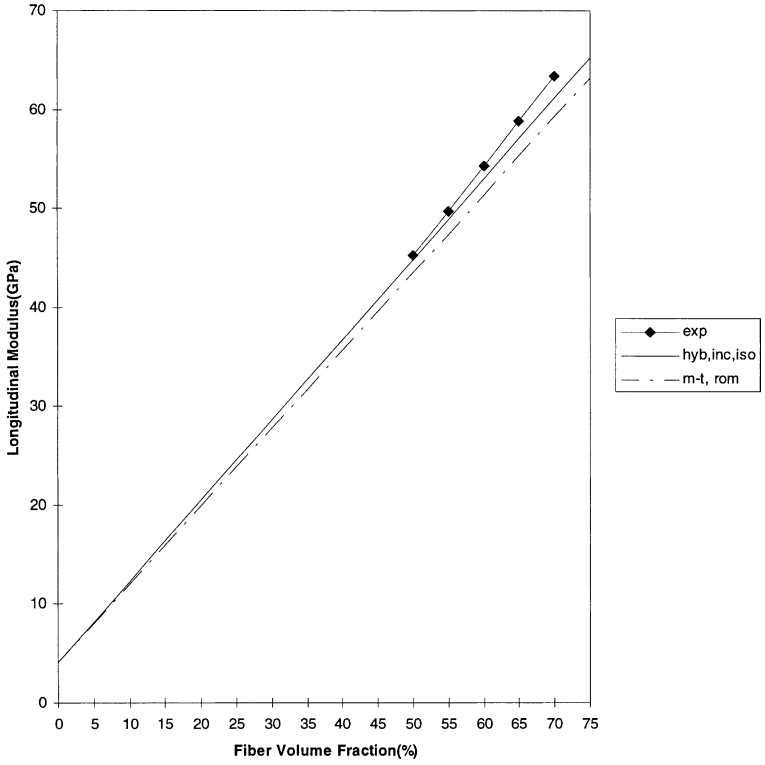

Fig. 3. The variations of longitudinal modulus with fiber volume fraction.

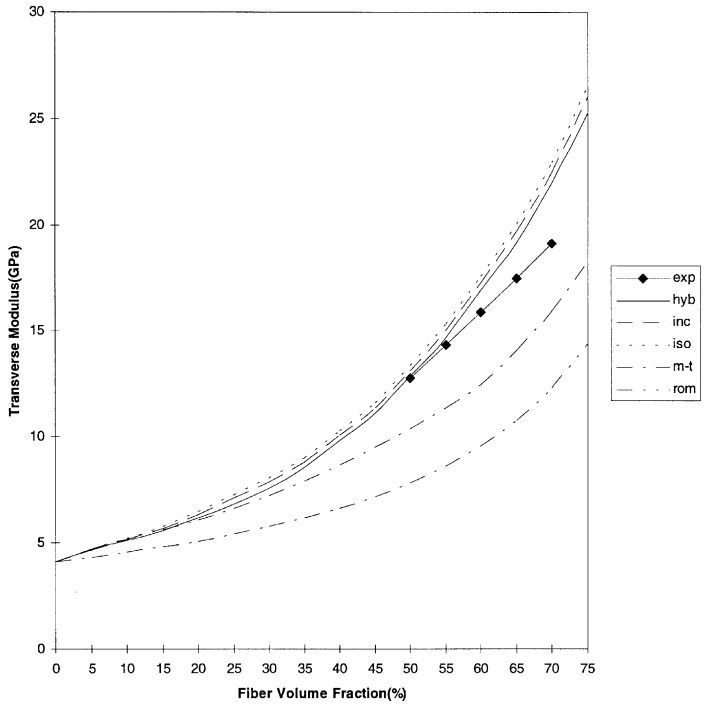

Fig. 4. The variations of transverse modulus with fiber volume fraction.

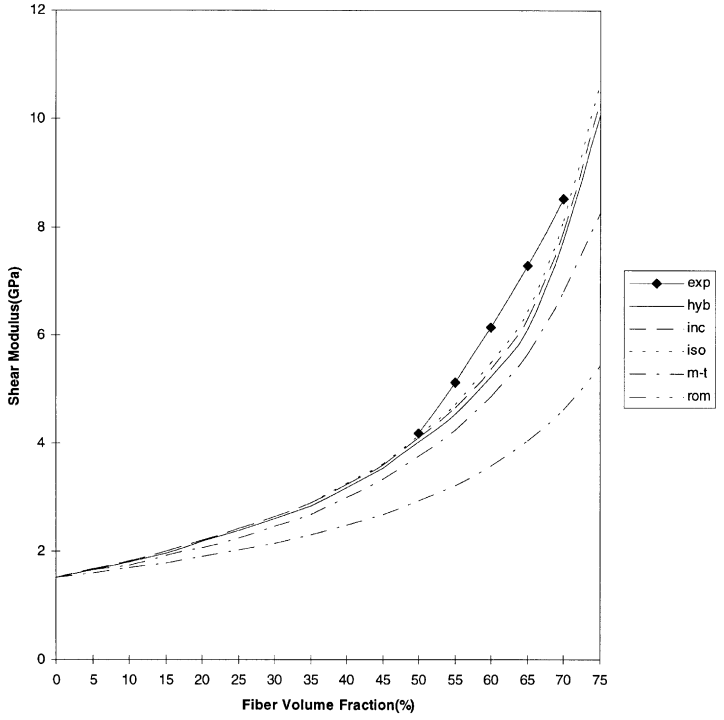

Fig. 5. The variations of shear modulus with fiber volume fraction.

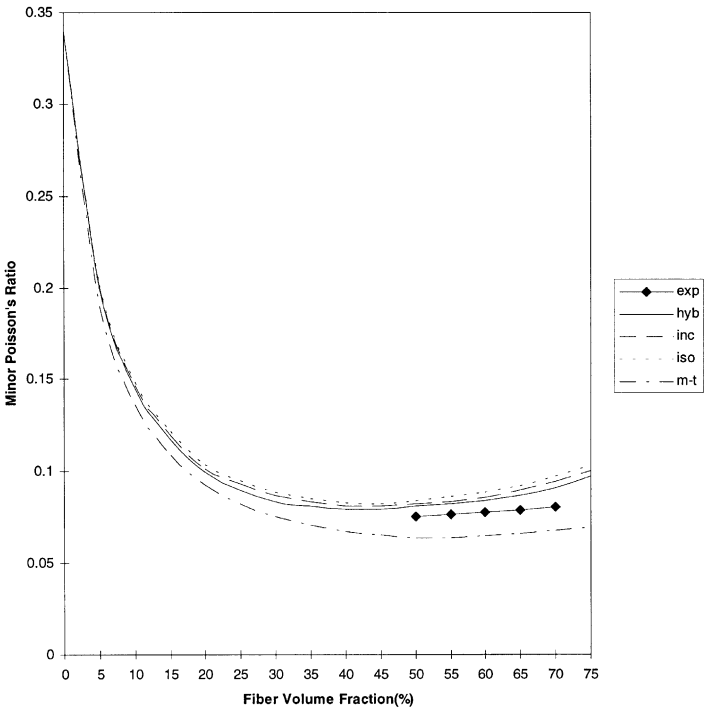

Fig. 6. The variations of minor Poisson's ratio with fiber volume fraction.

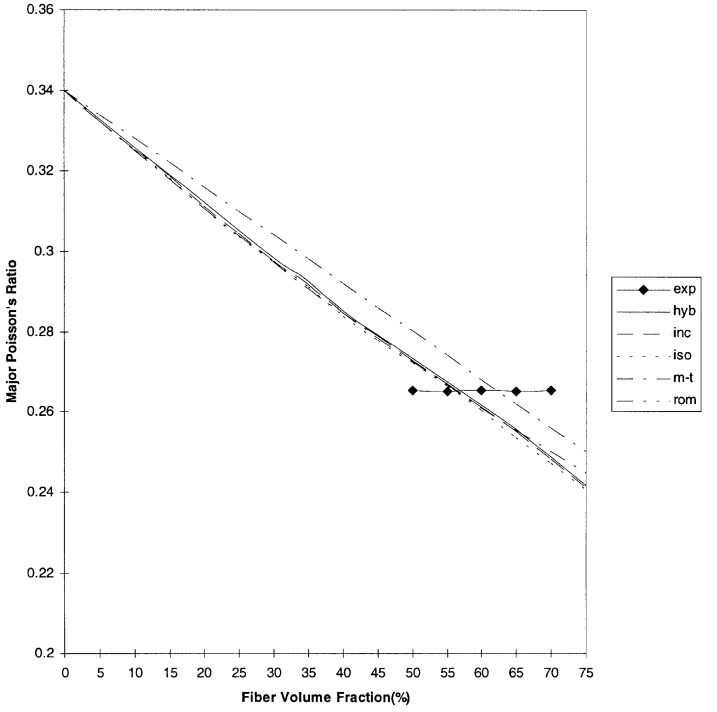

Fig. 7. The variations of major Poisson's ratio with fiber volume fraction.

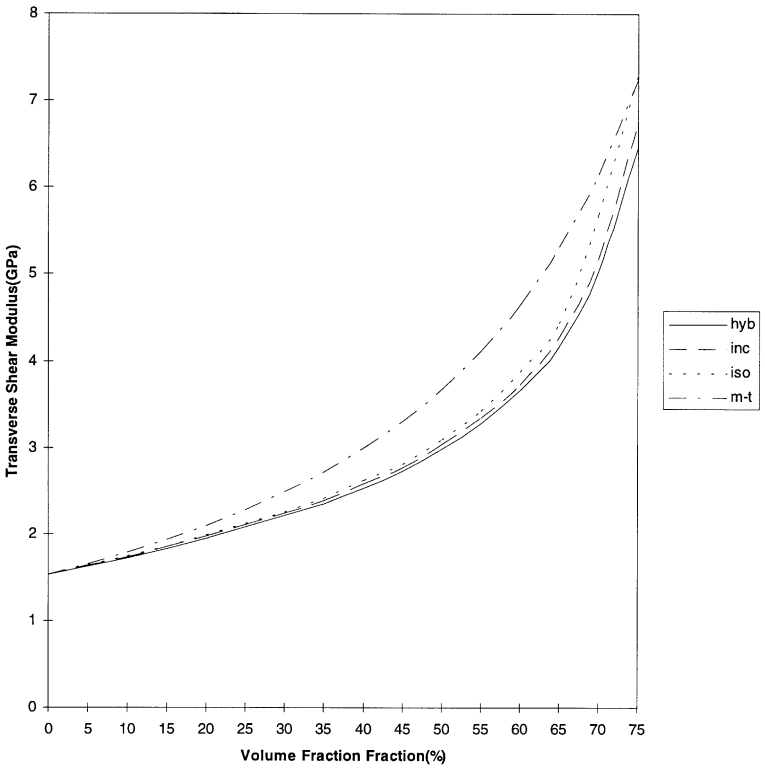

Fig. 8. The variations of transverse shear modulus with fiber volume fraction.

The numerical results by hybrid stress element are generally closest to the experimental results. The Mori–Tanaka method cannot give good results because Eshelby's tensor is based on the inclusion in an infinite matrix, which is of no reality in actual composite materials (Du and Wang, 1998).

6. Conclusions

The equivalent properties of composite materials with periodic microstructures are governed by a unit cell problem when the length scale of the microstructure is short in comparison to the length of global body.

Cooperating with homogenization method, the incompatible element and hybrid element have been developed to predict the mechanical behavior of composites. The incompatible element in this paper can pass the patch test condition. The hybrid stress element is constructed, based upon the consistency condition.

In contrast with the isoparametric displacement element, the incompatible element and hybrid element can ameliorate the results. Generally speaking, the numerical result by the hybrid element is the best comparing to the experimental result.

Further work based on the approach of multivariable finite element method proposed in this paper to three-dimensional case is being conducted by the authors, and will then be extended to the investigation of nonlinear performance of solids and structures, particularly the plasticity and fracture cases.

Acknowledgements

This work was supported by Australian Research Council and by National Natural Science Foundation of China (Grant No.: 19702016).

References

Clements, L.L., Moore, R.L., 1979. Composite properties for S-2 glass in a room-temperature-curable epoxy matrix. SAMPE Quarterly 10, 32–36.

Di, S.L., Wu, C.C., Song, Q.G., 1989. Model optimization of hybrid stress general shell element. Acta Mechanica Solida Sinica 2, 1–18.

Du, S.Y., Wang, B., 1998. Micromechanics of Composite Materials. Science Press, Beijing, pp. 41–42.

Hashin, Z., 1983. Analysis of composite materials – a survey. Journal of Applied Mechanics 50, 481–505.

Jansson, S., 1992. Homogenized nonlinear constitutive properties and local stress concentrations for composites with periodic internal structure. International Journal of Solids and Structures 29, 2181–2200.

Lee, J.A., Mykkanen, D.L., 1987. Metal and Polymer Matrix Composites. Noyes Data Corporation, NJ, p. 165.

Lene, F., 1986. Damage constitutive relations for composite materials. Engineering Fracture Mechanics 25, 713–728.

Lene, F., Leguillon, D., 1982. Homogenized constitutive law for a partially cohesive composite material. International Journal of Solids and Structures 18, 443–458.

Phan, N.D., Reddy, J.N., 1985. Analysis of laminated composite plates using a higher-order shear deformation theory. International Journal for Numerical Methods in Engineering 21, 2201–2219.

Pian, T.H.H., 1964. Derivation of element stiffness matrices by assumed stress distributions. AIAA Journal 2, 1333–1336.

Pian, T.H.H., Sumihara, K., 1984. Rational approach for assumed stress finite elements. International Journal for Numerical Methods in Engineering 20, 1685–1695.

Wu, C.C., Di, S.L., Huang, M.G., 1987. Optimization design of hybrid elements. Science Bulletin 32, 1236–1239.

Wu, C.C., Huang, M.G., Pian, T.H.H., 1987. Consistency condition and convergence criteria of incompatible elements: general formulation of incompatible functions and its application. Computers and Structures 27, 639–644.

Wu, C.C., Pian, T.H.H., 1997. Incompatible Numerical Analysis and Hybrid Element Method. Science Press, Beijing, pp. 45–105.

Zhao, Y.H., Weng, G.J., 1990. Effective elastic moduli of ribbon-reinforced composites. Journal of Applied Mechanics 57, 158–167.